

# A Reproducible Method for Mapping Electricity Transmission Infrastructure for Space Weather Risk Assessment

Edward J. Oughton<sup>1\*</sup>, Evan Alexander Peters<sup>1</sup>, Dennies Bor<sup>1</sup>, Noah Rivera<sup>1</sup>, C. Trevor Gaunt<sup>2</sup>, Robert Weigel<sup>1</sup>

<sup>1</sup>College of Science, George Mason University, Fairfax, VA, USA

<sup>2</sup>Dept. of Electrical Engineering, University of Cape Town, Cape Town, South Africa.

\*Corresponding author: Edward J. Oughton (e-mail: [eoughton@gmu.edu](mailto:eoughton@gmu.edu))

Address: College of Science, George Mason University, 4400 University Drive, Fairfax, VA

## Abstract

Space weather impact assessment is constrained by the lack of available asset information to undertake modeling of Geomagnetically Induced Currents (GICs) in Extra High Voltage electricity infrastructure networks. The U.S. National Space Weather Strategy and Action Plan identifies underutilized data as a central issue for improving risk assessment, motivating this research. Accurate GIC prediction is generally not possible without information on the electrical circuit, therefore we define a reproducible method based on open-source data, which enables risk analysts to collect their own substation component data. This process converts OpenStreetMap (OSM) substation locations to high-resolution, component-level mapping of electricity transmission assets by utilizing an innovative web-browser platform to facilitate component annotation. As a case study example, we convert an initial 1,313 high-voltage (>115 kV) substations to 52,273 substation components via Google Earth APIs utilizing low-altitude, satellite, and Streetview imagery. We find that a total of 41,642 substation components (79.6%) connect to the highest substation voltage levels (>345 kV) and are possibly susceptible to GIC, with a total of 7,949 transformers identified. Compared to the initial OSM baseline, we provide new detailed insights on voltage levels, line capacities, and substation configurations. Two validation workshops were undertaken to align the method and data with GIC assessment needs. The approach ensures consistency and rapid scalability, enabling users to quickly count components via a flexible web-browser application.

## Key Words

Mapping, Power System, Electricity Transmission, Critical Infrastructure, Space Weather, GIC

## 1. Introduction

There is grave concern about the threat of severe space weather affecting the critical infrastructure upon which we all rely, particularly for the ongoing operation of the power grid. Historical evidence indicates the possible impacts of Geomagnetically Induced Currents (GIC) on Extra High Voltage (EHV) electricity transmission infrastructure, leading to power system interruptions and collapse (blackouts), and transformer damage, motivating risk assessment to support mitigation decisions. Indeed, EHV transformers are expensive, hard to procure, and difficult to move. These assets are also challenging to repair or replace, highlighting possible supply chain difficulties. Currently there is already a global shortage in EHV transformers, with business-as-usual waiting times reported to be 2-3 years once ordered (Moseman, 2024). A global spike in demand for these assets, arising from a major space weather event, could cause considerable long-term disruption to society and the economy.

A wide variety of assessments have shown the potential economic impacts of an extreme event up to tens of billions of dollars of daily lost Gross Domestic Product (GDP) (Oughton, 2018; Oughton et al., 2017). The U.S. Government Accountability Office estimates a single GIC-induced blackout could cost up to \$1 billion to the U.S. economy, underscoring the importance of protecting critical infrastructure from space weather impacts (U.S. Government Accountability Office (GAO), 2018). Vulnerability to geomagnetic disturbances (GMD) is one of many hazards capable of degrading transmission assets through mechanical stresses and/or component failure, with the potential to cause large electricity outages (Kondrateva et al., 2020; Oughton et al., 2019; Verschuur et al., 2024). Consequently, there is an urgent need to map, model and pinpoint electricity transmission infrastructure vulnerabilities from natural hazards such as space weather, as identified by successive policy directives, such as via the U.S. National Space Weather Strategy (SWORM, 2023, 2019, 2015).

One approach over the past decade has been towards developing synthetic power networks which have broadly representative statistical characteristics to support modeling studies (Birchfield et al., 2017a, 2017b; Li et al., 2020; Xu et al., 2018). This research has been a step in the right direction, improving the types of data available to assess potential GIC impacts on electricity transmission infrastructure. However, this does not provide the ability for modelers to specifically understand hotspots of risk, and still leads to considerable uncertainty in identifying where to direct resources and research efforts nationally. Such strategic insight is absolutely required. Thus, our conjecture is that more data can still be collected from emerging geospatial data sources to improve our understanding of electrical transmission infrastructure, even if this only provides a partial understanding of the operational parameters in use (reducing uncertainty). Indeed, authoritative overviews of the methods for calculating GIC emphasize the importance of including appropriate power system characteristics for a modeled circuit, along with magnetic source fields and the present ground conductivity structure (Boteler and Pirjola, 2017). Once hotspots are identified, operational plans can be implemented relatively efficiently to mitigate vulnerabilities, protecting society and the economy (Mac Manus et al., 2023).

The developments in this paper offer new opportunities for refining electrical transmission network mapping and validation. By incorporating this approach, researchers can generate more accurate and detailed datasets, enhancing the potential for modeling and simulating critical power system infrastructure. This paper explores the following three research questions:

1. How does mapping EHV electricity transmission infrastructure at the component level enhance our understanding of GIC vulnerability in the U.S. transmission network?
2. What patterns in component distribution are observable within substation assets, and how do these vary by electrical asset classification?
3. How does this research methodology support reproducible expansion and refinement of OpenStreetMap (OSM) data in critical infrastructure mapping?

In the next section, we undertake a literature review, before articulating a reproducible methodology in Section 3 for collecting power network data using open-source imagery. In Section 4, results are then reported before returning in Section 5 to the research questions, discussing these within the broader context of the findings. Conclusions are provided in Section 6, along with identification of future research possibilities.

## 2. Literature Review

In this review an overview is provided of GIC impacts on the electricity transmission sector, as well as undertaking an evaluation of the range of geospatial data sources that could be used to supplement existing grid modeling approaches.

### 2.1. Reviewing the impacts of Geomagnetically Induced Currents (GICs)

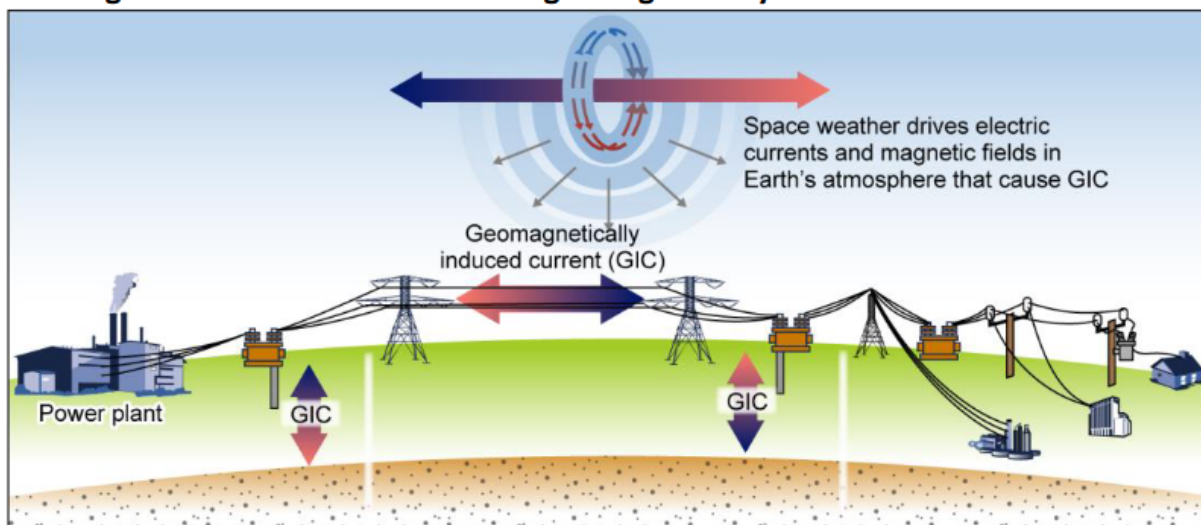
Space weather poses a significant risk to power grids and EHV transformers due to the creation of GICs, resulting from GMDs (Cordell et al., 2024; Smith et al., 2024; Vandegriff et al., 2024). Indeed, when Coronal Mass Ejections (CMEs) are thrown out from the Sun these huge releases of charged particles can interact with Earth's magnetic field, causing disturbances known as GMDs or solar storms (Lanabere et al., 2023; Liu et al., 2024; Owens et al., 2021). The disturbances of the magnetosphere and ionosphere induce electric fields within Earth's surface, leading to low-frequency GICs flowing into conductive networks such as electricity transmission infrastructure (Ingham et al., 2023; Ngwira et al., 2023; Pratscher et al., 2024). Indeed, localized geoelectric field peaks during geomagnetic storms can exceed regional averages by over 100%, suggesting how regionally nuanced this threat poses to specific transmission grid assets (Ngwira et al., 2015). Such variability in geoelectric fields highlights the need for spatially precise modeling to understand transformer vulnerabilities.

Power systems support the functionality of all other infrastructure systems, highlighting their importance (Hall et al., 2017, 2016). Generally, the GICs a power grid can be exposed to are highly dependent on the voltage, configuration, length and spatial direction of the network (Andreyev et al., 2023). Traditionally, higher latitude locations were considered as having the largest exposure to GIC, although more recently research has shown that substations located in high ground resistivity areas or near long transmission lines experience heightened GIC impact due to stronger induced geoelectric fields (Barnes et al., 2024; Kazerooni et al., 2017). This emphasizes the importance of understanding the three-dimensional Earth conductivity structure in Earth's crust when trying to model GICs (Espinosa et al., 2023; Marshalko et al., 2023; Nakamura et al., 2018). In terms of network configuration, longer and higher voltage transmission lines tend to conduct higher GICs, with the potential to flow into substations and increase vulnerability to space weather (Caraballo et al., 2023; Kazerooni et al., 2017). Susceptibility can also vary by orientation, with transmission lines parallel to the Earth's magnetic field being up to several times more affected by

GICs than those oriented perpendicular to it, leading to uneven impacts across the grid (Mayer and Stork, 2024).

As GICs flow through power transmission systems, critical components such as EHV transformers are especially exposed because they have low resistance to DC-like currents, such as GICs, and can cause saturation of the transformer's core, leading to inefficient operation and overheating (Ahmadzadeh-Shooshtari and Rezaei-Zare, 2022a; Subritzky et al., 2024). Three main mechanisms of failure from GICs are identified. Firstly, prolonged saturation can damage transformer windings, leading to permanent failure from transformer heating (Akbari et al., 2023; Akbari and Rezaei-Zare, 2023; Albert et al., 2022). Secondly, inefficient power delivery, often referred to as excessive reactive power being drawn from the grid, can lead to voltage instability, potentially leading to a voltage collapse (Saleh et al., 2024). Thirdly, harmful harmonics can be produced that can affect grid operations (Ahmadzadeh-Shooshtari and Rezaei-Zare, 2022b; Crack et al., 2024) and cause important components such as transformers to trip, removing an asset from normal operation (Dimmock et al., 2024). There is concern that any of these mechanisms can lead to a GIC-induced cascading failure with widespread power outages, as seen during the 1989 Quebec blackout. This reinforces the critical importance and motivation for collecting detailed component-level data on transformers and other substation components. Without such granularity into the circuit design, it becomes difficult to predict how specific assets may respond under stress.

### Geomagnetic disturbances can lead to geomagnetically induced current.



Sources: GAO (presentation); Art Explosion (images). | GAO-19-98

Figure 1 Space weather impacts on power grid components due to GICs

## 2.2. Using Geospatial Data to Identify and Map Infrastructure Assets

There is growing interest in using geospatial information to identify and map infrastructure assets. Such information can then be used improve the accuracy of existing models that simulate both normal operating conditions and disruptions caused by external factors, such as GMDs. By utilizing geospatial data, it is possible to precisely locate and appraise the characteristics of infrastructure components, such as transformers, powerlines, and reactors for electric grid assets. Although some power operators have highly

sophisticated asset tracking and management systems, the durable lifespan of some of these operating assets mean they were initially deployed many decades ago. Subsequently, the data collection methods reviewed here can also be utilized network operators to readily map and appraise their own assets, such as for monitoring asset operational condition.

Within power systems, there is a shift towards tracking information on assets by combining geospatial data with remote sensing to monitor key characteristics (Fechner et al., 2020). Indeed, remote sensing data has become a valuable resource for energy infrastructure mapping due to its affordability, availability, and accessibility, even in remote regions (Ren et al., 2022). Manual surveying sites in-person can be expensive and time-consuming, requiring the surveyor to physically travel to each location. Although all network lines and substations will have been surveyed prior to construction, not all information may have made its way into a modern asset management platform, such as a Building Information Management (BIM) platform, or for use in a more advanced ‘digital twin’ of the ongoing network (Ghenai et al., 2022; Loggia and Flamini, 2024). Thus, remotely sensing asset performance and condition is therefore an attractive option (Ahmed et al., 2022), especially to populate new decision-support modeling approaches with necessary data.

Efforts to classify power grid components using remote sensing have advanced significantly, leveraging satellite imagery and public data sources (Plaen et al., 2024). One such example employs a combination of satellite imagery and LiDAR-enabled point cloud detection algorithms to extract transformer information from publicly available data (Arastounia and Lichti, 2015). Previous studies have emphasized the importance of high-resolution imaging in remote sensing, arguing that spatial resolutions between 0.25 and 1 meter are necessary to capture small but significant infrastructure elements like utility lines and transformers (Jensen and Cowen, 2011). In cases of more visually prominent features, resolutions of 1.5 to 10 meters as provided by SPOT6/7, and Sentinel-2 are adequate for mapping a global database of transmission components (Kruitwagen et al., 2021). Lower-resolution imagery often results in misclassification or overlooked assets, which is critical when managing urban utility infrastructure and must be front of mind when designing an asset annotation system. For context, a single high-resolution Ortho-imagery study detected over 19,000 distributed Photo-Voltaic (PV) arrays across four cities, demonstrating the importance of detailed spatial data for accurate infrastructure mapping in solar energy installations (Bradbury et al., 2016).

Incorporating geospatial data into modeling efforts bridges the gap between manual and automated classification, providing a more accurate understanding of the grid’s structure. Machine learning algorithms can improve classification efficiency and accuracy, essential for large-scale mapping projects. Machine learning has already enabled automated extraction of transmission line and substation data from remotely sensed imagery, streamlining data acquisition (Ren et al., 2022). Studies also demonstrate how convolutional neural networks can automate infrastructure mapping, providing a scalable solution to detect assets, supporting component level detection capabilities. By reducing reliance on exhaustive manual input for classification, machine learning can expand datasets for infrastructure resilience modeling (Bradbury et al., 2016).

To refine and scale annotation methods for infrastructure mapping, machine learning techniques trained on manually-annotated coordinate-based details can enhance accuracy and efficiency. For example,

coordinate-based data in LiDAR point clouds support accurate automated-recognition of substation transformers (Arastounia and Lichti, 2015). Moreover, the effectiveness of location-specific training data in aerial electrical system mapping shows that using coordinate-level granularity enables automated models to align component details with geospatial information, enhancing both identification accuracy and dataset integration potential. Research has been completed at a global scale using remote sensing and machine learning to identify and map a comprehensive dataset of 68,661 PV installations across 131 countries. The approach uses high-resolution satellite imagery (1.5-meter to 10-meter resolution) balancing spatial accuracy with spectral sensitivity, effectively capturing PV arrays' spectral signature and installation footprint. The study processed a search area of 72.1 million square kilometers, covering nearly half of Earth's land surface, and resulted in a global installed capacity estimate of 423 gigawatts as of 2018 (Kruitwagen et al., 2021). Provided the technology is available, scale is only limited by necessary computational resources, and the committed willingness of human participants to validate estimated results.

Engaging crowdsourcing platforms like OSM allow for community-based data collection, filling gaps in remote sensing datasets with local observations. Recent assessment demonstrates the effectiveness of crowdsourcing in mapping solar PV installations, where volunteer-contributed annotation enhanced dataset coverage at the street level (Stowell et al., 2020). Public contributions improve infrastructure data by adding local insights (Bradbury et al., 2016).

While automated methods can process large datasets quickly, they often struggle with precision in complex or heterogeneous environments. Challenges in capturing intricate equipment configurations during classification occurs when automated systems struggle with accurately recognizing complex substation components, particularly in settings with intricate geometric primitives like cylindrical and planar surfaces (Arastounia and Lichti, 2015). Examples include identifying and distinguishing between 3-phase transformers, banks of three 1-phase transformers, and reactors. Vertical connections between circuit segments crossing others are not visible and must be identified in other ways, while it is impossible to determine the open/closed state of circuit breakers. Manual methods are often needed to accurately identify and interpret these complexities reliably, as automated recognition may fall short due to poor segmentation and interpretation (e.g., due to poor image resolution) (Blaschke, 2010; Zanotta et al., 2018). By reducing the risk of misidentification in low-resolution imagery, manual classification and validation can improve the potential quality of final data.

### 3. Methodology

We now present a systematic approach for refining OSM data granularity to achieve high-resolution, component-level mapping of electricity substation assets. The methodology is organized into three main phases, including Step A. Technical Software Design and Data Integration, Step B. Initial Asset Annotation Approach and Step C. Refinement and Validation. By integrating multiple data sources and a browser-enabled classification environment, we develop a comprehensive component-level dataset designed for improving GIC assessment.

#### 3.1. Step A. Technical Software Design and Data Integration

Substation location data are sourced from OSM, yielding a dataset of approximately 60,000 generation, distribution, and transmission substations. These substations are categorized into their Federal Energy

Regulatory Commission (FERC) grid regions to define their geographical and operational boundaries. Transmission line data are obtained from the Homeland Infrastructure Foundation-Level Data (HIFLD) and geospatially intersected to identify lines connecting to the substations. High-voltage transmission lines and substations rated at 230 kV and above are specifically filtered, as these systems are susceptible to GICs due to their minimal resistance to GIC path flows.

A custom annotation web interface is then developed using the Google Maps Static Application Programming Interface (API). This tool integrates workflows that enable users to identify and characterize substation components. The web interface is supported by a Python-based server hosted on the Amazon Web Services (AWS) cloud platform and synchronized with a relational database system (AWS RDS). For each grid region, substations are listed on the web dashboard, which upon user selection, retrieves Google Earth imagery of the substation. Users can also inspect, annotate, and validate components using Google Street View imagery, if accessible. Only authorized users can update, label, and save data, ensuring secure and controlled data management. Additionally, users can toggle transmission lines intersecting with specific substations, enabling precise mapping and analysis.

This platform allows both technical and non-technical users to access and annotate data collaboratively, enabling real-time updates, and facilitating data entry and interaction with substation assets. The data framework is tailored to substation assets, classified by visual properties such as category and subcategory. Comparative parameters, including geospatial detail, voltage estimations, operational function, and component interconnections, are established to ensure consistent standards across data sources. This standardization allows for efficient data organization and prepares the dataset for annotation and analysis in Geographic JavaScript Object Notation (GeoJSON) or Comma Separated Value (CSV) formats.



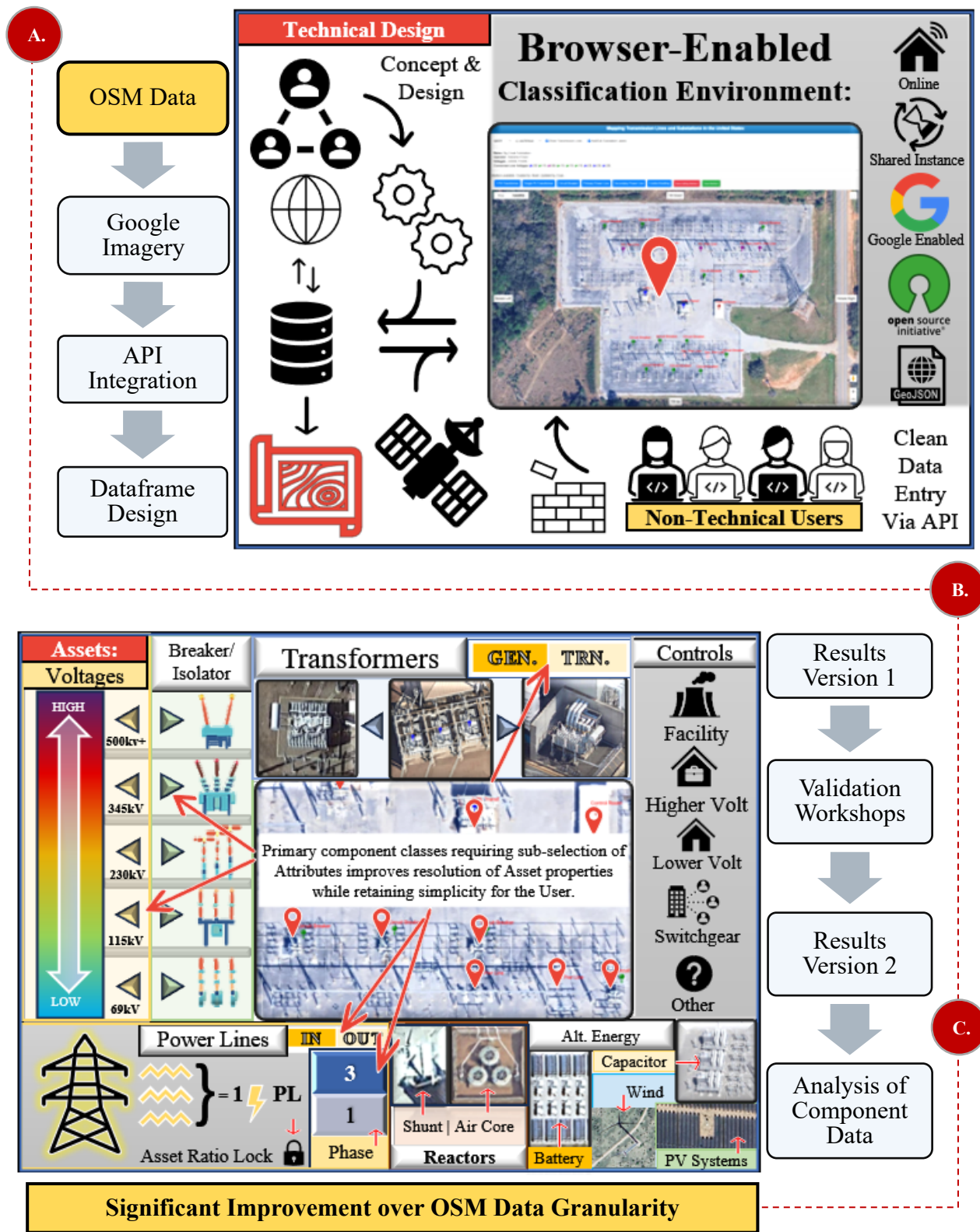


Figure 2 A method for identifying relevant transmission assets for GIC assessment



### 3.2. Step B. Initial Asset Annotation Approach

Individual components within each substation are annotated independently in the browser-enabled environment, including transformers, transmission line connections, circuit breakers, controls, and alternative energy sources. These marker labels include both the component type as well as additional observable attributes such as phase, utility, and relative voltage category, effectively creating subtypes for enhancing analysis. An initial asset dataset is established, consisting of a single-user annotation for all 1,313 available OSM substations (>115 kV). Each component is visually identified and labeled based on observable features, ensuring that the dataset accurately captures the full range of substation infrastructure components to establish a measurable baseline for assessing correct or incorrect categorization, as illustrated in Figure 3. This approach also allows for the adjustment of entire classifications due to normalized discrepancies in subject matter labeling, rather than consistency of recognition.

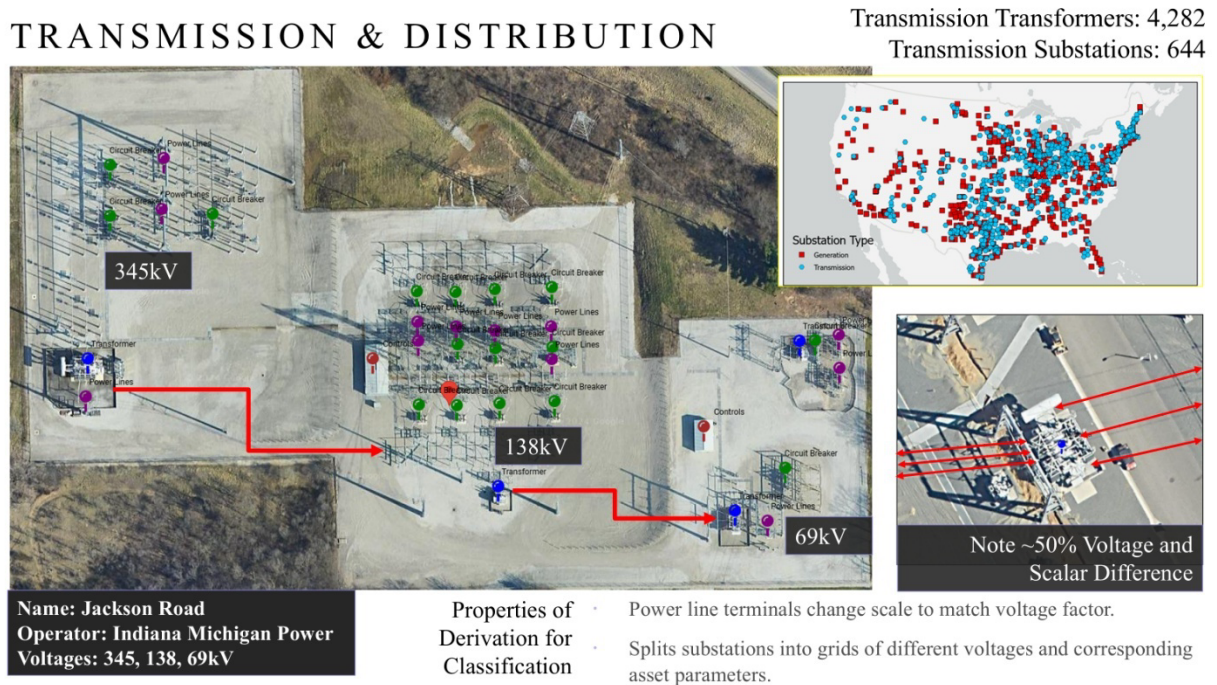


Figure 3 Voltage Mapping by Spatial Configuration.

### 3.3. Step C. Refinement and Validation

After the initial labeling of assets, further classifications are identified, as illustrated for generation transformers in Figure 4. While transformers are the key assets relevant to GIC assessment, circuit breakers are also readily identifiable as some types are visually distinct in appearance and configuration. Three main types are defined here, including Type 1 (1-phase, dead-tank) which handle the relatively highest voltage within a substation ( $\geq 345$  kV). Next, Type 2 (3-phase, dead tank) is the second highest, ranging from 230 kV to 345 kV. Finally, Type 3 (banks of 1-phase live tank) ranges from 115 kV up to 230 kV. Lower voltage circuit breakers may be possible to identify, although image resolution to enable classification of these smaller assets may be inconsistent (as only urban areas have the highest resolution imagery in Google Earth). For circuit breakers and proximate isolators and transformers, voltage values are assigned based on initial image classification and phase spacing, and consistency between the connected objects. These iterative refinements ensure the collected data not only capture the nuances of substation infrastructure but

also aligned with operational and modeling requirements for assessing resilience to geomagnetic disturbances.

## POWER GENERATION

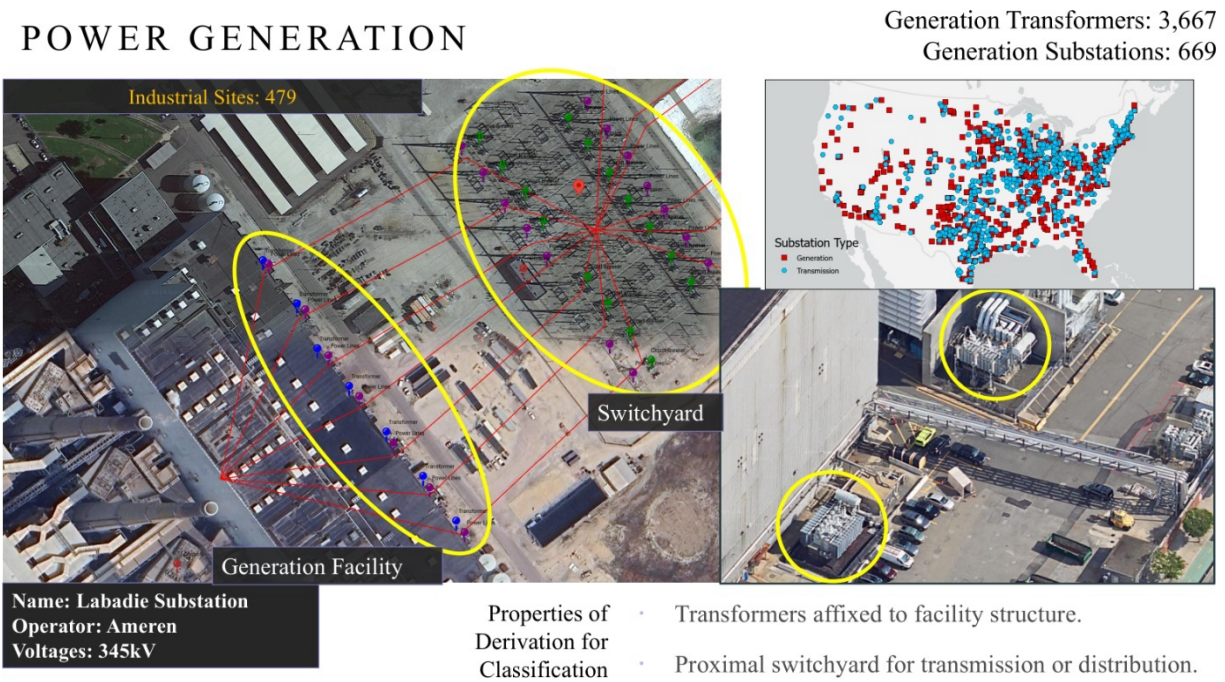


Figure 4 Refining areas of interest for specific component classes, such as generation transformers.

Two validation workshops are then undertaken with domain experts to support dataset refinement and ensure accuracy. The first consists of specialists in electrical transmission networks for a comprehensive review of the dataset. This includes attendees who have extensive experience in operating these assets and undertaking GIC assessment, as well as those with expert backgrounds in smart grids and power system design. The aim is to help both refine and validate transformer and circuit breaker annotations based on operational and spatial relationships. The workshop consists of describing the method, and then presenting classified substation components from the first tranche of labeled components. The second workshop provides a detailed review of the dataset’s applicability for GIC modeling and grid resilience planning by space weather experts from the natural sciences (e.g., physics). A similar approach is proposed, whereby the overall method steps are described, followed by an articulation of the component-labeling categories in use. These workshops collectively refine the method to ensure (i) component labels are being applied correctly, and (ii) the correct information is being collected for GIC assessment, delivering quality assurance, validation and relevancy. After the workshops, any inconsistencies in the data labeling approach are corrected, to produce a single finalized set of components.

## 4. Results

Here we report the results using the United States as a case study example. After eliminating duplicates and limiting distance-based component inclusion per substation, the U.S. dataset is refined to a sample of 1,313 outdoor substation assets with 52,273 annotated components, providing a robust foundation for detailed infrastructure analysis and modeling. In this section we cover the regions of interest, and produce visualizations of the collected data, particularly with reference to the proportional composition of

components across the three substation voltage categories considered. Figure 5 reports the different regional transmission planning units and independent system operators for the contiguous U.S., in accordance with FERC Order No. 1000. These provide natural boundaries for the networks in question.

At the highest level, the U.S. electricity grid is divided into three regions: Western, Eastern, and the Texas Electricity Reliability Council of Texas (ERCOT). Although these regions are electrically independent, efforts have been made to create redundant connections to mitigate grid-wide downtime in case of voltage collapse. Further down the hierarchy are local independent producers and distributors of electricity. FERC allows these operators to pool resources and form Independent System Operators (ISOs) functioning in smaller regions such as states or counties.

These ISOs may operate independently or collaborate as Regional Transmission Planning (RTP) operators. FERC's role is to regulate and ensure a non-discriminatory power supply to consumers through RTOs. Here, 14 electricity grid regions under FERC Order No. 1000 policy are considered and illustrated in Figure 4. The Texas grid (ERCOT), although not governed within the policy's scope, is also addressed as an RTO.

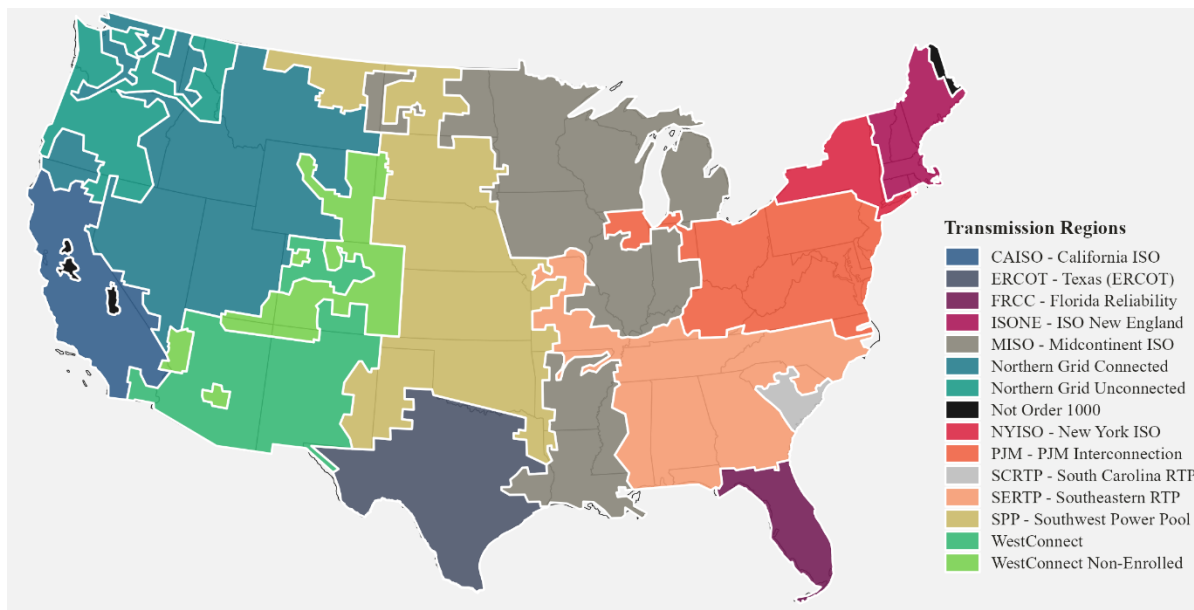


*Figure 5 Regional Transmission Planning and Independent System Operators. These regions have been digitized in accordance with FERC Order No. 1000.*

In Figure 6 a-c, we visualize the granularity of substation locations. In Figure 6 d-f substations are characterized by their voltage handling capacities, divided into three classes: Medium Voltage (115 to 230 kV), High Voltage (230 to 345 kV), and Ultra High Voltage (345 to 750 kV), a necessary simplification to deal with the observable variations at most substations and the mono-typing of the overall EHV class in electricity transmission systems. For each region, an average maximum voltage is calculated by summing the highest voltage values observed for each substation and dividing by the number of substations in that region. In the research dataset, the average maximum voltage is derived by averaging the high and low voltage values for each of the 52,273 components, rounded to one decimal place. Each substation's overall

voltage type is classified based on the highest voltage observed in its components to reflect exposure to voltage ranges.

Figure 6 g-I, shows the number of line connections to each substation. OSM data contain a single category for line connections, while the research dataset differentiates internal lines connected within the source substation. Line capacity is categorized based on connection count quantiles of the OSM data as follows: connections below the first quartile are classified as "Low," those between the first and third quartiles as "Medium," and connections in the top quartile as "High".

In Figure 7 the number of annotated substation components are reported by region. The total component count is calculated by summing all component labels in all substations and is a representation of the effort to increase resolution for modeling.



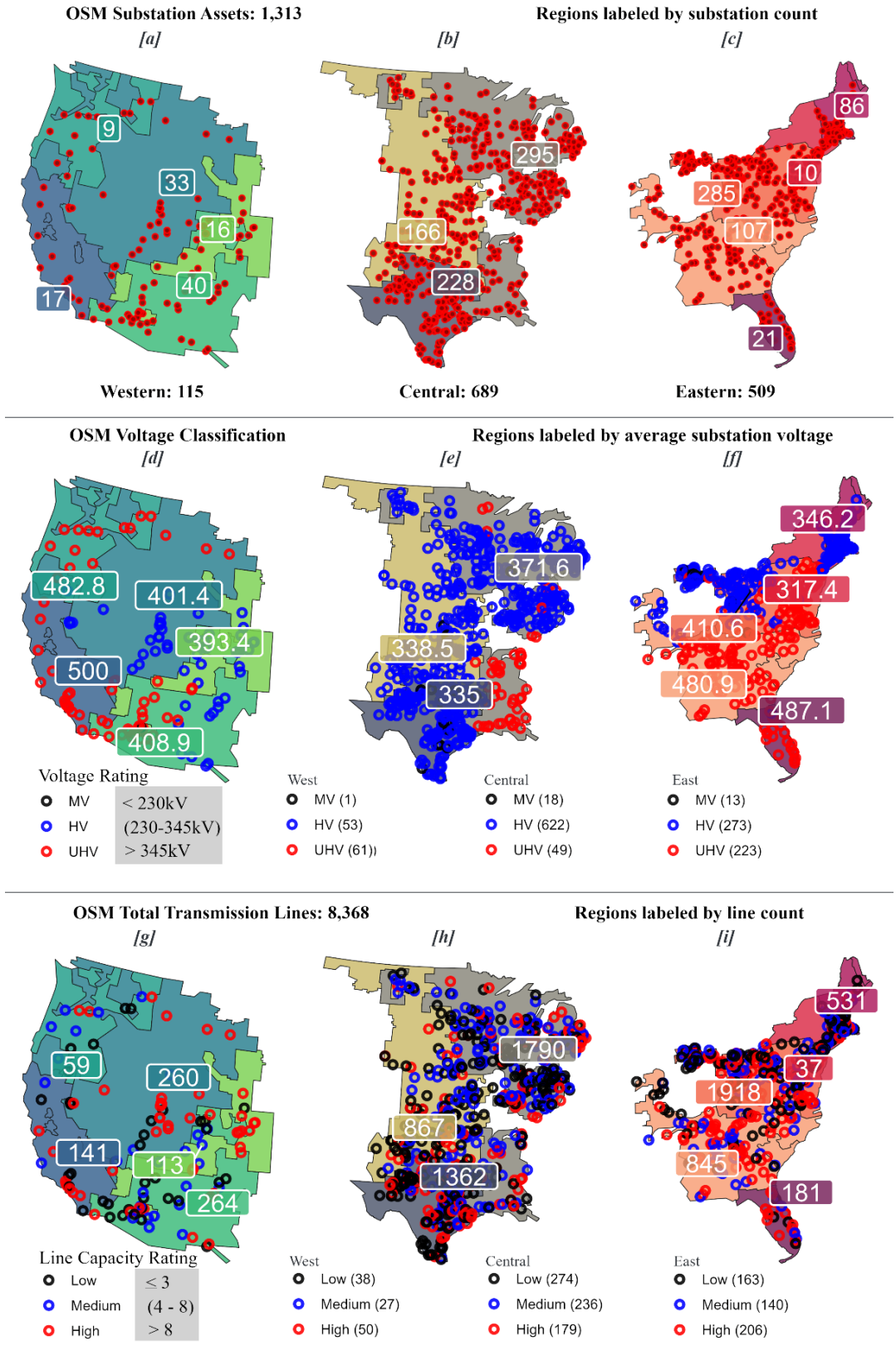


Figure 6 Analysis on OSM data prior to integration of annotated components.

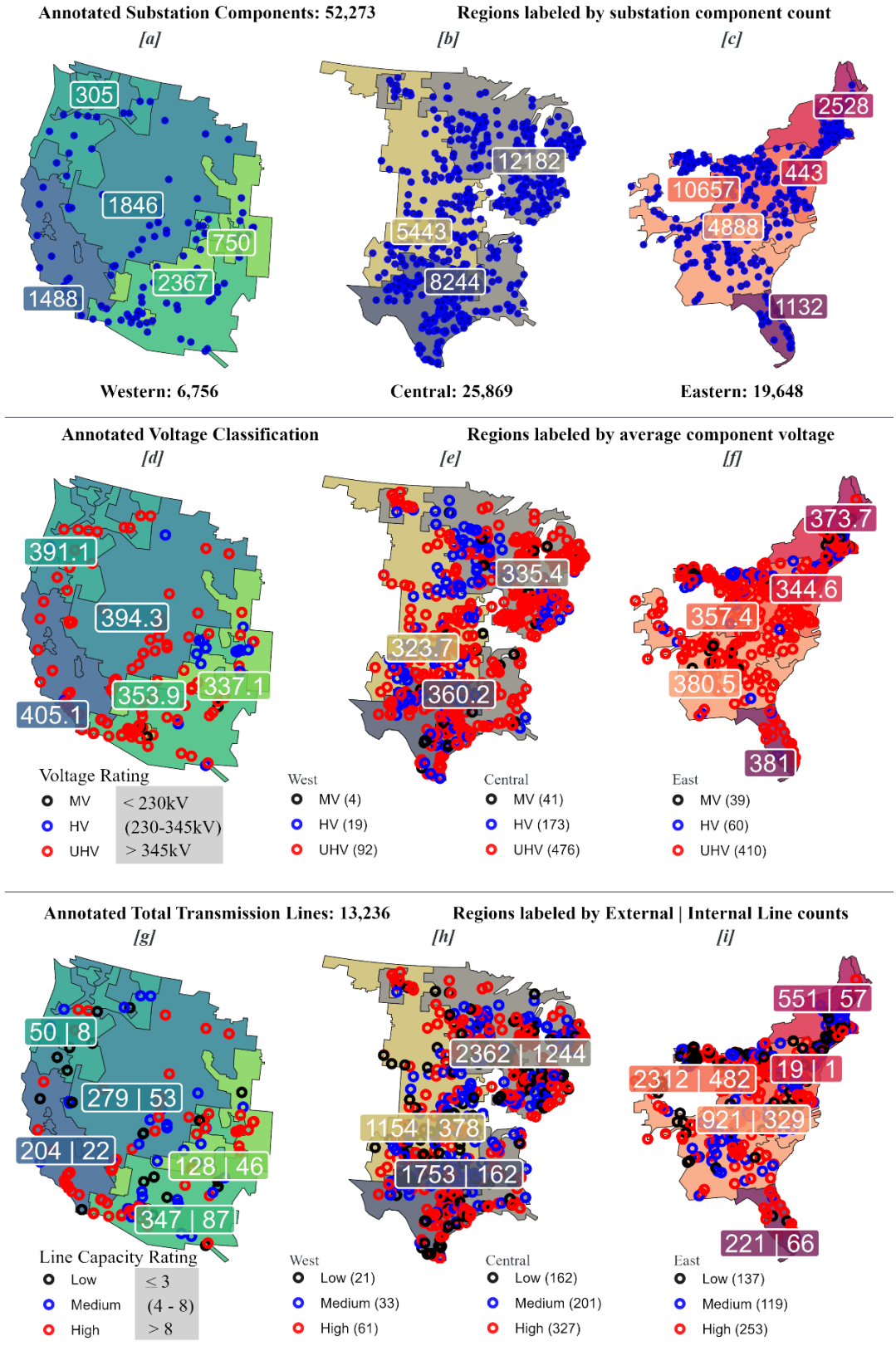


Figure 7 Analysis of complete annotated research data.



Components	52,273	Substation Voltage Rating Type			1,313 Substations
Alt. Energy	2,457	MV	HV	UHV	Proportion
Battery	1293	6.01%	5.11%	4.55%	4.70%
Solar	732	36.21%	17.08%	61.97%	52.63%
Wind	432	33.62%	30.34%	29.43%	29.79%
<b>Circuit Breaker</b>	<b>20,794</b>	30.17%	52.58%	8.60%	17.58%
HV CB	5307	<b>28.05%</b>	<b>40.14%</b>	<b>40.25%</b>	<b>39.78%</b>
MV CB	9185	100.00%	50.87%	40.97%	44.17%
UHV CB	6302	0.00%	49.13%	21.43%	25.52%
<b>Controls</b>	<b>2,931</b>	0.00%	0.00%	37.60%	30.31%
Industrial	479	<b>7.67%</b>	<b>5.88%</b>	<b>5.45%</b>	<b>5.61%</b>
Lower Voltage	961	8.78%	16.99%	16.69%	16.34%
Switchgear	424	41.89%	32.03%	32.36%	32.79%
Upper Voltage	1067	29.05%	12.50%	13.96%	14.47%
<b>Isolation Asset</b>	<b>3,331</b>	20.27%	38.48%	36.99%	36.40%
Arrestor	1037	<b>10.32%</b>	<b>6.31%</b>	<b>6.20%</b>	<b>6.37%</b>
Capacitor	1492	55.28%	38.80%	27.64%	31.13%
Disconnect	802	24.62%	35.15%	48.39%	44.79%
<b>Power Lines</b>	<b>13,236</b>	20.10%	26.05%	23.96%	24.08%
External	10301	<b>28.62%</b>	<b>26.58%</b>	<b>24.91%</b>	<b>25.32%</b>
Internal	2935	87.50%	77.22%	77.45%	77.83%
<b>Reactors</b>	<b>1,575</b>	12.50%	22.78%	22.55%	22.17%
Air Core	1346	<b>3.11%</b>	<b>2.78%</b>	<b>3.06%</b>	<b>3.01%</b>
Shunt	229	95.00%	90.50%	84.05%	85.46%
<b>Transformer</b>	<b>7,949</b>	5.00%	9.50%	15.95%	14.54%
Gen 1	916	<b>16.23%</b>	<b>13.19%</b>	<b>15.58%</b>	<b>15.21%</b>
Gen 3	2751	10.86%	5.57%	12.61%	11.52%
Trans 1	1532	27.48%	41.55%	33.72%	34.61%
Trans 3	2750	21.41%	9.84%	20.84%	19.27%
		40.26%	43.03%	32.83%	34.60%

Table 1 Asset and component counts with proportional representation across substation voltage types

Table 1 presents the composition of substation components across the three projected voltage categories. Each percentage represents the proportion of that component type within the specific voltage category. The final column, "Total," shows the overall contribution of each component type as a percentage of all components across all substations. This breakdown highlights the distribution of each component type by voltage classification, providing insight into the proportional roles these assets play within substations of different voltage levels. It helps identify trends, such as the concentration of certain components in particular voltage types, which is useful for assessing infrastructure configurations and vulnerabilities.

## 5. Discussion

Having outlined the methodology for collecting component-level substation data, and reported results for the case study example of the United States, we now return to the research questions.

*How does mapping high-voltage infrastructure at the component level enhance our understanding of GIC vulnerability in the electricity transmission network?*

The enhanced component-level mapping in this study provides significant insights into GIC vulnerabilities by introducing a more granular and accurate dataset for infrastructure analysis. The methodology increased identified UHV substations across all regions, reflecting a critical improvement in data resolution based on component design. Due to the desire to understand which locations may be susceptible to GIC, substations were classified by the highest voltage present. In the Western region, UHV substations increased from 61 in the OSM dataset to 92 in the new data, representing a 51% increase. In the Central region, UHV substations rose from 49 to 476, a substantial 871% increase. Finally, in the high-risk Eastern region, UHV substations grew from 223 to 410, an 84% increase. These improvements are particularly impactful in regions like the Eastern U.S., where reported ground conductivity structure, latitude and coastal proximity factors amplify GIC exposure. Accurately identifying these assets enables targeted resilience strategies, including prioritization of transformer and circuit breaker upgrades in vulnerable locations.

A key advancement of this study is the extensive documentation of circuit breakers, which account for 40% of all components, or 20,794 in total. Circuit breakers are distributed across voltage categories, with 44% in Medium Voltage (MV), 26% in High Voltage (HV), and 30% in Ultra-High Voltage (UHV). Importantly, in our first iteration the break points were assigned by statistical observations in the OSM information, though the voltage ranges assigned to the visual classifications can be reparametrized to provide more regional specificity. This somewhat even distribution reflects the utility of managing voltage flow across substation assets and ensuring operational stability throughout fluctuations in grid layouts.

The study also sheds significant light on the number and type of present transformers, which make up 15% of the total components, or 7,949 in total. These are classified into generation and transmission types, with generation transformers comprising 46% and transmission transformers comprising 54% of the total. This classification splits substations evenly into "generation" sites (those with generation transformers present) and "transmission" sites (lacking generation transformers). This near 50/50 split highlights the dual functional roles of substations within the network, with generation sites playing a unique role in grid resilience by producing power independently. Transmission substations, meanwhile, focus on managing and routing electricity across the network, often concentrating on HV (230-345 kV) and UHV (>345kV) operations. Three-phase transformers dominate the transformer category - the HV and UHV classifications, with significant concentrations at these voltage levels to meet the demands of high-capacity systems.

In summary, the refined dataset provides a substantial improvement in component-level detail, enabling more nuanced analysis of GIC vulnerabilities across U.S. electricity transmission networks. This work can support the development of targeted resilience measures, ensuring critical assets such as transformers are prioritized and the power system safeguarded against GMDs.

*What patterns in component distribution are observable within substation assets, and how do these vary by apparatus classification?*

The component-level mapping achieved in this study demonstrates a dramatic increase in granularity, offering a more detailed perspective on substation infrastructure than previously available. The OSM dataset, which represented 1,313 assets, has been expanded to include 52,273 individual components in the new research dataset, an increase in resolution of nearly 3,880%. This substantial growth in detail enables concentrated analysis of asset distribution and electrical apparatus classification across regions and voltage levels, uncovering patterns that were previously obscured, but are highly important for GIC vulnerability assessment. Indeed, the increased granularity is evident across all regions. For example, in the Western

region, resolution expanded from 115 in the OSM dataset to 6,756, a 5,794% increase. Similarly, the Central region grew by 3,654% (from 689 assets to 25,869 components), while the Eastern region saw a 3,761% increase (from 509 to 19,648). These improvements highlight the enhanced resolution of the research dataset, allowing for a more detailed examination of substation infrastructure. Moreover, at the regional subset level, similar patterns emerged. CAISO in the Western subset saw an 8,647% increase (from 17 assets in OSM to 1,488 components). In the Eastern subset, SERTP recorded a 4,468% increase (from 107 to 4,888 components), demonstrating the dataset's enhanced ability to capture assets in areas of operational and infrastructural importance. These improvements in detail provide a way to develop more comprehensive network assessments of transmission infrastructure, reducing model uncertainty, particularly in regions critical to the stability of the grid.

The dataset also reveals patterns in voltage averages, with adjustments that may provide a more accurate depiction of operational conditions. In the Western region, average maximum voltage values declined significantly, reflecting a correction of possible prior overestimations. For instance, NGUC's average voltage dropped from 483 kV in OSM to 391 kV, and CAISO's average voltage decreased from 500 kV to 405 kV, a reduction of 18-22%. Similarly, WCNE experienced a decline from 393 kV to 337 kV. These adjustments indicate that the OSM dataset overestimates operational voltages, likely due to insufficient granularity in distinguishing lower-voltage assets within substations, especially when considering the overall rise in substations with UHV connections. In contrast, the Central region displayed mixed results. For example, ERCOT's average voltage increased from 335 kV to 360 kV, reflecting the inclusion of previously unclassified HV infrastructure, while MISO and SPP saw declines. MISO dropped from 372 kV to 335 kV, and SPP from 339 kV to 324 kV, indicating a more refined understanding of HV and UHV configurations. The Eastern region exhibited a balance of increases and decreases. Subsets like ISONE and NYISO saw average voltage rises, with ISONE increasing from 346 kV to 374 kV and NYISO from 317 kV to 345 kV. Meanwhile, PJM and SERTP experienced reductions, with PJM declining from 411 kV to 357 kV and SERTP from 481 kV to 381 kV. These adjustments may align the dataset more closely with actual infrastructure conditions, creating a more accurate representation of voltage levels across regions.

Line capacities showed significant changes, with a total increase of 58% across all regions compared to the OSM dataset. Reclassification of substation line capacities revealed distinct regional patterns. In the Western region, low-capacity substations decreased from 38 to 21, while high-capacity substations increased from 50 to 61. In the Central region, the changes were even more pronounced. Low-capacity substations decreased from 274 to 162, while high-capacity substations surged from 179 to 327, reflecting the region's role as a heavily connected transmission hub. These adjustments illustrate the Central region's capacity to handle large power flows. In the Eastern region, similar trends were observed. Low-capacity substations decreased from 163 to 137, and high-capacity substations increased from 206 to 253. These reclassifications underscore the Eastern region's dense industrial and urban infrastructure, where high-capacity substations are critical to meeting demand.

Mapping alternative energy components reveals distinct roles for batteries, solar panels, and wind turbines across voltage categories. Battery systems are concentrated at UHV substations, comprising 62% of alternative energy components within this category. At HV and MV substations, batteries account for 17% and 36%, respectively, emphasizing their critical role as energy reserves for high-capacity infrastructure. Overall, batteries contribute 53% to the alternative energy category. Solar PV generating stations are evenly distributed, accounting for 34% of alternative energy components at MV substations, 30% at HV, and 29% at UHV.

*How does this research methodology support reproducible expansion and refinement of OSM data in critical infrastructure mapping?*

The methodology developed in this study establishes a strong foundation for enhancing the accuracy and scope of infrastructure mapping based on OSM data. By leveraging publicly available imagery and integrating it with a browser-enabled platform, the approach allows for systematic, high-resolution data collection that is accessible, iterative, and capable of refinement over time. The open-source nature of OSM makes it particularly suitable as a baseline resource for collaboration among researchers, utilities, and public agencies, providing a scalable and adaptable framework for critical infrastructure analysis.

This study's detailed component-level data on transformers, transmission lines, and other substation assets demonstrates the potential to significantly refine the granularity and utility of mapping based on OSM's baseline datasets. With over 52,273 components mapped across 1,313 substations, the results provide a comprehensive snapshot of current infrastructure, highlighting areas for further refinement and expansion. Continued iterations of this methodology can address gaps in substation layouts, component granularity, and voltage classifications, enabling more detailed mapping of infrastructure such as lower voltage ranges in regional and local transmission networks. The feedback loop introduced in this research merges refined annotations with coordinate-specific classifications and supplementary information, improving internal dataset accuracy and relevance. This iterative process allows the dataset to evolve over time, adapting to new findings while maintaining alignment with operational priorities and research needs.

Although not directly relevant for GIC assessment, many lower-voltage substations remain unaccounted for or may be under-analyzed. The techniques developed in this study offer a practical means to address these gaps, enhancing our understanding of lower voltage network structure. This is indirectly relevant when a power outage occurs at a higher voltage substation (e.g., from GIC), as when cascading failure occurs it would be useful to know which areas are likely to be affected or not at lower voltage substations.

## 6. Conclusion

This study set out to provide a generalizable, reproducible methodology for collecting EHV substation component data to enable improved GIC assessment. Here, we use the U.S. as a case study example, substantially enhancing the granularity and accuracy of electricity transmission assets compared to what is currently available. For example, by focusing on improving substation asset data for modeling and resilience planning, we leveraged publicly available imagery and annotations integrated with OSM data to create a high-resolution, component-level dataset. Spanning 52,273 individual components, this dataset categorizes critical components important for GIC vulnerability assessment, such as transformers, circuit breakers, and transmission lines, offering a detailed view of substation configurations. The resulting methodology not only improves data accuracy but also provides a robust foundation for scalable, collaborative mapping efforts. This framework supports the development of infrastructure models that are essential for analyzing vulnerabilities, including those linked to GMDs, while contributing to the broader goal of enhancing infrastructure resilience. The method can be readily applied to other countries.

The quantitative findings highlight the improvements achieved through this approach. Regional resolution of geolocated assets increased dramatically, reflecting enhancements in the identification of items that can parameterize the functionality and structure of electricity transmission substations. The Western region experienced a 5,794% increase in identified components (from 115 in OSM to 6,756), while the Central

and Eastern regions saw increases of 3,654% (from 689 to 25,869) and 3,761% (from 509 to 19,648), respectively. These substantial improvements demonstrate the ability of the new dataset to capture a more granular view of substation assets. Notably, the identification of UHV linked substations (>345 kV) nearly doubled in high-risk regions, such as the Eastern subset, where counts rose from 223 in OSM data to 410 in the research dataset. Voltage classification methods regionally analyze statistical estimations, with average maximum voltages in NGUC and CAISO regions reduced by 18-22%, despite the considerable increase in overall UHV voltage type assets. With a better understanding of substation line capacities and possible connection points, these findings highlight the potential of the enhanced dataset to support more accurate infrastructure parameterization, enabling improved GIC risk assessments, reduced uncertainty, and shifting towards more predictive appraisals.

Despite these advancements, limitations were identified that present opportunities for future research. Individual transmission lines are heavily reliant on imagery of the highest resolution. Due to this impact of distortion and lack of clarity, tracing the exact pathway of transmission lines was avoided and instead the focus was on the substation circuitry that permits connections. The absence of burial tags for underground conduits constrained the accuracy of mapping in urban regions like NYISO, where buried infrastructure is more significant. This limitation restricted the study's ability to fully represent transmission networks in densely populated areas. This constraint was also observed by the low count of power lines in the OSM data as well. Additionally, while the dataset provides a static snapshot of component configurations, the lack of dynamic operational data limits its capacity to model real-time network behavior. Regarding methodology, there is an opportunity in the current application of voltage assignments, which were treated homogeneously in this study, to provide a more tailored perspective. Future research should focus on extracting more specific circuit breaker operating voltages according to attributes such as region, operator, or manufacturer information and rerunning the analysis to refine component assignments further.

This research supports the broader application of open-source mapping approaches to improve assessment models. By emphasizing collaborative data collection, the project enables the rapid development of detailed models, particularly relevant for studying geomagnetic disturbances and other specific risks to critical infrastructure. While this study prioritized isolating component data points that are considered most vulnerable to GICs, it also tracked components that may not directly relate to GICs but hold value for broader risk modeling. These efforts ensure that the dataset is versatile, providing opportunities for infrastructure operators to enhance system integrity.

### Acknowledgements

This material is based upon work supported by the NSF National Center for Atmospheric Research, which is a major facility sponsored by the U.S. National Science Foundation under Cooperative Agreement No. 1852977. The project upon which this article is based was funded through the NSF NCAR Early-Career Faculty Innovator Program under the same Cooperative Agreement. We also gratefully acknowledge funding from the ChronoStorm NSF RAPID grant (#2434136), co-funded by the GEO/AGS Space Weather Research and the ENG/CMMI Humans, Disasters, and the Built Environment programs.

### References

Ahmadzadeh-Shooshtari, B., Rezaei-Zare, A., 2022a. A Waveform-Based Approach for Transformer Differential Protection Under GIC Conditions. *IEEE Trans. Power Deliv.* 37, 5366–5375. <https://doi.org/10.1109/TPWRD.2022.3176815>

- Ahmadzadeh-Shoostari, B., Rezaei-Zare, A., 2022b. Advanced Transformer Differential Protection Under GIC Conditions. *IEEE Trans. Power Deliv.* 37, 1433–1444. <https://doi.org/10.1109/TPWRD.2021.3087463>
- Ahmed, MD.F., Mohanta, J.C., Sanyal, A., 2022. Inspection and identification of transmission line insulator breakdown based on deep learning using aerial images. *Electr. Power Syst. Res.* 211, 108199. <https://doi.org/10.1016/j.epsr.2022.108199>
- Akbari, M., Mostafaei, M., Rezaei-Zare, A., 2023. Estimation of Hot-Spot Heating in OIP Transformer Bushings Due to Geomagnetically Induced Current. *IEEE Trans. Power Deliv.* 38, 1277–1285. <https://doi.org/10.1109/TPWRD.2022.3212322>
- Akbari, M., Rezaei-Zare, A., 2023. Thermal Analysis of Power Transformers Under Geomagnetically Induced Current. *IEEE Trans. Power Deliv.* 38, 4114–4121. <https://doi.org/10.1109/TPWRD.2023.3303106>
- Albert, D., Schachinger, P., Bailey, R.L., Renner, H., Achleitner, G., 2022. Analysis of Long-Term GIC Measurements in Transformers in Austria. *Space Weather* 20, e2021SW002912. <https://doi.org/10.1029/2021SW002912>
- Andreyev, A.B., Mukasheva, S.N., Kapytin, V.I., Sokolova, O.I., 2023. Estimating Geomagnetically Induced Currents in High-Voltage Power Lines for the Territory of Kazakhstan. *Space Weather* 21, e2023SW003639. <https://doi.org/10.1029/2023SW003639>
- Arastounia, M., Lichti, D.D., 2015. Automatic Object Extraction from Electrical Substation Point Clouds. *Remote Sens.* 7, 15605–15629. <https://doi.org/10.3390/rs71115605>
- Barnes, A.K., Mate, A., Bent, R., 2024. A Review of the GIC Blocker Placement Problem. <https://doi.org/10.48550/arXiv.2402.07302>
- Birchfield, A.B., Gegner, K.M., Xu, T., Shetye, K.S., Overbye, T.J., 2017a. Statistical Considerations in the Creation of Realistic Synthetic Power Grids for Geomagnetic Disturbance Studies. *IEEE Trans. Power Syst.* 32, 1502–1510. <https://doi.org/10.1109/TPWRS.2016.2586460>
- Birchfield, A.B., Schweitzer, E., Athari, M.H., Xu, T., Overbye, T.J., Scaglione, A., Wang, Z., 2017b. A Metric-Based Validation Process to Assess the Realism of Synthetic Power Grids. *Energies* 10, 1233. <https://doi.org/10.3390/en10081233>
- Blaschke, T., 2010. Object based image analysis for remote sensing. *ISPRS J. Photogramm. Remote Sens.* 65, 2–16. <https://doi.org/10.1016/j.isprsjprs.2009.06.004>
- Boteler, D.H., Pirjola, R.J., 2017. Modeling geomagnetically induced currents. *Space Weather* 15, 258–276. <https://doi.org/10.1002/2016SW001499>
- Bradbury, K., Saboo, R., L. Johnson, T., Malof, J.M., Devarajan, A., Zhang, W., M. Collins, L., G. Newell, R., 2016. Distributed solar photovoltaic array location and extent dataset for remote sensing object identification. *Sci. Data* 3, 160106. <https://doi.org/10.1038/sdata.2016.106>
- Caraballo, R., González-Esparza, J.A., Pacheco, C.R., Corona-Romero, P., 2023. Improved Model for GIC Calculation in the Mexican Power Grid. *Space Weather* 21, e2022SW003202. <https://doi.org/10.1029/2022SW003202>
- Cordell, D., Mann, I.R., Parry, H., Unsworth, M.J., Cui, R., Clark, C., Kelemen, E., MacMullin, R., 2024. Modeling Geomagnetically Induced Currents in the Alberta Power Network: Comparison and Validation Using Hall Probe Measurements During a Magnetic Storm. *Space Weather* 22, e2023SW003813. <https://doi.org/10.1029/2023SW003813>
- Crack, M., Rodger, C.J., Clilverd, M.A., Mac Manus, D.H., Martin, I., Dalzell, M., Subritzky, S.P., Watson, N.R., Petersen, T., 2024. Even-Order Harmonic Distortion Observations During Multiple Geomagnetic Disturbances: Investigation From New Zealand. *Space Weather* 22, e2024SW003879. <https://doi.org/10.1029/2024SW003879>
- Dimmock, A.P., Lanabere, V., Johlander, A., Rosenqvist, L., Yordanova, E., Buchert, S., Molenkamp, S., Setréus, J., 2024. Investigating the Trip of a Transformer in Sweden During the 24 April 2023 Storm. *Space Weather* 22, e2024SW003948. <https://doi.org/10.1029/2024SW003948>



- Espinosa, K.V., Padilha, A.L., Alves, L.R., Schultz, A., Kelbert, A., 2023. Estimating Geomagnetically Induced Currents in Southern Brazil Using 3-D Earth Resistivity Model. *Space Weather* 21, e2022SW003166. <https://doi.org/10.1029/2022SW003166>
- Fechner, H., Johnston, W., Masson, G., Altenhöfer-Pflaum, G., Tilli, F., Hüsser, P., Haghdadi, N., Bründlinger, R., Frederiksen, K.H.B., Heilscher, G., Graditi, G., Adinolfi, G., Ueda, Y., Guerrero Lemus, R., Bucher, C., Mather, B., 2020. Data Model for PV Systems - Data Model and Data Acquisition for PV registration schemes and grid connection evaluations – Best Practice and Recommendations (info:eu-repo/semantics/report), Fechner, H.; Johnston, W.; Masson, G.; Altenhöfer-Pflaum, G.; Tilli, F.; Hüsser, P.; Haghdadi, N.; Bründlinger, R.; Frederiksen, K.H.B.; Heilscher, G.; Graditi, G.; Adinolfi, G.; Ueda, Y.; Guerrero Lemus, R.; Bucher, C.; Mather, B. (2020). Data Model for PV Systems - Data Model and Data Acquisition for PV registration schemes and grid connection evaluations – Best Practice and Recommendations (IEA PVPS Task 14). IEA PVPS Task 14. IEA PVPS Task 14.
- Ghenai, C., Husein, L.A., Al Nahlawi, M., Hamid, A.K., Bettayeb, M., 2022. Recent trends of digital twin technologies in the energy sector: A comprehensive review. *Sustain. Energy Technol. Assess.* 54, 102837. <https://doi.org/10.1016/j.seta.2022.102837>
- Hall, J.W., Thacker, S., Ives, M.C., Cao, Y., Chaudry, M., Blainey, S.P., Oughton, E.J., 2017. Strategic analysis of the future of national infrastructure. *Proc. Inst. Civ. Eng. - Civ. Eng.* 170, 39–47. <https://doi.org/10.1680/jcien.16.00018>
- Hall, J.W., Tran, M., Hickford, A.J., Nicholls, R.J., 2016. The future of national infrastructure: A system-of-systems approach. Cambridge University Press.
- Ingham, M., Pratscher, K., Heise, W., Bertrand, E., Kruglyakov, M., Rodger, C.J., 2023. Influence of Tectonic and Geological Structure on GIC in Southern South Island, New Zealand. *Space Weather* 21, e2023SW003550. <https://doi.org/10.1029/2023SW003550>
- Jensen, J.R., Cowen, D.C., 2011. Remote Sensing of Urban/Suburban Infrastructure and Socio-Economic Attributes, in: Dodge, M., Kitchin, R., Perkins, C. (Eds.), *The Map Reader*. Wiley, pp. 153–163. <https://doi.org/10.1002/9780470979587.ch22>
- Kazerooni, M., Zhu, H., Overbye, T.J., 2017. Improved Modeling of Geomagnetically Induced Currents Utilizing Derivation Techniques for Substation Grounding Resistance. *IEEE Trans. Power Deliv.* 32, 2320–2328. <https://doi.org/10.1109/TPWRD.2016.2616399>
- Kondrateva, O., Myasnikova, E., Loktionov, O., 2020. Analysis of the Climatic Factors Influence on the Overhead Transmission Lines Reliability. *Rigas Teh. Univ. Zinat. Raksti Vides Un Klimata Tehnol.* 13 Ser. 24, 201–214. <https://doi.org/10.2478/rtuect-2020-0097>
- Kruitwagen, L., Story, K.T., Friedrich, J., Byers, L., Skillman, S., Hepburn, C., 2021. A global inventory of photovoltaic solar energy generating units. *Nature* 598, 604–610. <https://doi.org/10.1038/s41586-021-03957-7>
- Lanabere, V., Dimmock, A.P., Rosenqvist, L., Juusola, L., Viljanen, A., Johlander, A., Odelstad, E., 2023. Analysis of the Geoelectric Field in Sweden Over Solar Cycles 23 and 24: Spatial and Temporal Variability During Strong GIC Events. *Space Weather* 21, e2023SW003588. <https://doi.org/10.1029/2023SW003588>
- Li, H., Wert, J.L., Birchfield, A.B., Overbye, T.J., Roman, T.G.S., Domingo, C.M., Marcos, F.E.P., Martinez, P.D., Elgindy, T., Palmintier, B., 2020. Building Highly Detailed Synthetic Electric Grid Data Sets for Combined Transmission and Distribution Systems. *IEEE Open Access J. Power Energy* 7, 478–488. <https://doi.org/10.1109/OAJPE.2020.3029278>
- Lindahl, J., Johansson, R., Lingfors, D., 2023. Mapping of decentralised photovoltaic and solar thermal systems by remote sensing aerial imagery and deep machine learning for statistic generation. *Energy AI* 14, 100300. <https://doi.org/10.1016/j.egyai.2023.100300>
- Liu, T.Z., Shi, X., Hartinger, M.D., Angelopoulos, V., Rodger, C.J., Viljanen, A., Qi, Y., Shi, C., Parry, H., Mann, I., Cordell, D., Madanian, H., Mac Manus, D.H., Dalzell, M., Cui, R., MacMullin, R., Young-Morris, G., Noel, C., Streifling, J., 2024. Global Observations of Geomagnetically

- Induced Currents Caused by an Extremely Intense Density Pulse During a Coronal Mass Ejection. *Space Weather* 22, e2024SW003993. <https://doi.org/10.1029/2024SW003993>
- Loggia, R., Flamini, A., 2024. Electrical Safety Enhanced With BIM, SCADA and Digital Twin Integration: A Case Study of a MV-LV Substation. *IEEE Trans. Ind. Appl.* 60, 2725–2731. <https://doi.org/10.1109/TIA.2023.3332311>
- Mac Manus, D.H., Rodger, C.J., Renton, A., Ronald, J., Harper, D., Taylor, C., Dalzell, M., Divett, T., Clilverd, M.A., 2023. Geomagnetically Induced Current Mitigation in New Zealand: Operational Mitigation Method Development With Industry Input. *Space Weather* 21, e2023SW003533. <https://doi.org/10.1029/2023SW003533>
- Marshalko, E., Kruglyakov, M., Kuvshinov, A., Viljanen, A., 2023. Three-Dimensional Modeling of the Ground Electric Field in Fennoscandia During the Halloween Geomagnetic Storm. *Space Weather* 21, e2022SW003370. <https://doi.org/10.1029/2022SW003370>
- Mayer, D., Stork, M., 2024. Sciendo. *J. Electr. Eng.* 75, 224–228. <https://doi.org/10.2478/jee-2024-0027>
- Moseman, A., 2024. Transformer Shortage Crisis: Can New Engineering Solve It? - IEEE Spectrum [WWW Document]. URL <https://spectrum.ieee.org/transformer-shortage> (accessed 12.17.24).
- Nakamura, S., Ebihara, Y., Fujita, S., Goto, T., Yamada, N., Watari, S., Omura, Y., 2018. Time Domain Simulation of Geomagnetically Induced Current (GIC) Flowing in 500-kV Power Grid in Japan Including a Three-Dimensional Ground Inhomogeneity. *Space Weather* 16, 1946–1959. <https://doi.org/10.1029/2018SW002004>
- Ngwira, C.M., Arritt, R., Perry, C., Weygand, J.M., Sharma, R., 2023. Occurrence of Large Geomagnetically Induced Currents Within the EPRI SUNBURST Monitoring Network. *Space Weather* 21, e2023SW003532. <https://doi.org/10.1029/2023SW003532>
- Ngwira, C.M., Pulkkinen, A.A., Bernabeu, E., Eichner, J., Viljanen, A., Crowley, G., 2015. Characteristics of extreme geoelectric fields and their possible causes: Localized peak enhancements. *Geophys. Res. Lett.* 42, 6916–6921. <https://doi.org/10.1002/2015GL065061>
- Oughton, E.J., 2018. The Economic Impact of Critical National Infrastructure Failure Due to Space Weather. *Oxf. Res. Encycl. Nat. Hazard Sci.* <https://doi.org/10.1093/acrefore/9780199389407.013.315>
- Oughton, E.J., Ralph, D., Pant, R., Leverett, R., Copic, J., Thacker, S., Dada, R., S., S., Tuveson, M., Hall, J.W., 2019. Stochastic Counterfactual Risk Analysis for the Vulnerability Assessment of Cyber-Physical Attacks on Electricity Distribution Infrastructure Networks. *Risk Anal.* 39, 2012–2031. <https://doi.org/10.1111/risa.13291>
- Oughton, E.J., Skelton, A., Horne, R.B., Thomson, A.W.P., Gaunt, C.T., 2017. Quantifying the daily economic impact of extreme space weather due to failure in electricity transmission infrastructure. *Space Weather* 15, 65–83. <https://doi.org/10.1002/2016SW001491>
- Owens, M.J., Lockwood, M., Barnard, L.A., Scott, C.J., Haines, C., Macneil, A., 2021. Extreme Space-Weather Events and the Solar Cycle. *Sol. Phys.* 296, 82. <https://doi.org/10.1007/s11207-021-01831-3>
- Plaen, J.J.-F.G.D., Koks, E.E., Ward, P.J., 2024. Towards an open pipeline for the detection of critical infrastructure from satellite imagery—a case study on electrical substations in The Netherlands. *Environ. Res. Infrastruct. Sustain.* 4, 035009. <https://doi.org/10.1088/2634-4505/ad63c9>
- Pratscher, K.M., Ingham, M., Mac Manus, D.H., Kruglyakov, M., Heise, W., Rodger, C.J., Divett, T., Bertrand, E., Dalzell, M., Brundell, J., 2024. Modeling GIC in the Southern South Island of Aotearoa New Zealand Using Magnetotelluric Data. *Space Weather* 22, e2024SW003907. <https://doi.org/10.1029/2024SW003907>
- Ren, S., Hu, W., Bradbury, K., Harrison-Atlas, D., Malaguzzi Valeri, L., Murray, B., Malof, J.M., 2022. Automated Extraction of Energy Systems Information from Remotely Sensed Data: A Review and Analysis. *Appl. Energy* 326, 119876. <https://doi.org/10.1016/j.apenergy.2022.119876>
- Saleh, S.A., Zundel, E.W., Young-Morris, G., Meng, J., Cardenas, J., Hill, E.F.S., Brown, S., 2024. Impacts of Transformer Loading on the Harmonic Distortion Created by GIC Flows. *IEEE Trans. Ind. Appl.* 60, 4666–4676. <https://doi.org/10.1109/TIA.2024.3362924>

- Smith, A.W., Rodger, C.J., Mac Manus, D.H., Rae, I.J., Fogg, A.R., Forsyth, C., Fisher, P., Petersen, T., Dalzell, M., 2024. Sudden Commencements and Geomagnetically Induced Currents in New Zealand: Correlations and Dependence. *Space Weather* 22, e2023SW003731. <https://doi.org/10.1029/2023SW003731>
- Stowell, D., Kelly, J., Tanner, D., Taylor, J., Jones, E., Geddes, J., Chalstrey, E., 2020. A harmonised, high-coverage, open dataset of solar photovoltaic installations in the UK. *Sci. Data* 7, 394. <https://doi.org/10.1038/s41597-020-00739-0>
- Subritzky, S.P., Laphorn, A.C., Hardie, S., Manus, D.H.M., Rodger, C.J., Dalzell, M., 2024. Assessment of Space Weather Impacts on New Zealand Power Transformers Using Dissolved Gas Analysis. *Space Weather* 22, e2023SW003607. <https://doi.org/10.1029/2023SW003607>
- SWORM, 2023. White paper on the implementation status of the national space weather strategy and action plan. Space Weather Operations, Research, and Mitigation Subcommittee, Washington D.C.
- SWORM, 2019. National space weather strategy and action plan. Executive Office of the President of the United States, Washington D.C.
- SWORM, 2015. National space weather strategy and action plan. Executive Office of the President of the United States, Washington D.C.
- U.S. Government Accountability Office (GAO), 2018. TECHNOLOGY ASSESSMENT Critical Infrastructure Protection Protecting the Electric Grid from Geomagnetic Disturbances.pdf [WWW Document]. URL <https://www.gao.gov/assets/700/696284.pdf> (accessed 10.12.24).
- Vandegriff, E.M., Welling, D.T., Mukhopadhyay, A., Dimmock, A.P., Morley, S.K., Lopez, R.E., 2024. Exploring Localized Geomagnetic Disturbances in Global MHD: Physics and Numerics. *Space Weather* 22, e2023SW003799. <https://doi.org/10.1029/2023SW003799>
- Verschuur, J., Fernández-Pérez, A., Mühlhofer, E., Nirandjan, S., Borgomeo, E., Becher, O., Voskaki, A., Oughton, E.J., Stankovski, A., Greco, S.F., Koks, E.E., Pant, R., Hall, J.W., 2024. Quantifying climate risks to infrastructure systems: A comparative review of developments across infrastructure sectors. *PLOS Clim.* 3, e0000331. <https://doi.org/10.1371/journal.pclm.0000331>
- Xu, T., Birchfield, A.B., Overbye, T.J., 2018. Modeling, Tuning, and Validating System Dynamics in Synthetic Electric Grids. *IEEE Trans. Power Syst.* 33, 6501–6509. <https://doi.org/10.1109/TPWRS.2018.2823702>
- Zanotta, D.C., Zortea, M., Ferreira, M.P., 2018. A supervised approach for simultaneous segmentation and classification of remote sensing images. *ISPRS J. Photogramm. Remote Sens.* 142, 162–173. <https://doi.org/10.1016/j.isprsjprs.2018.05.021>